Engineering Geology 294 (2021) 106321

Contents lists available at ScienceDirect

Engineering Geology

journal homepage: www.elsevier.com/locate/enggeo

An experimental investigation of shear strength behavior of a welded bimrock by meso-scale direct shear tests

Elif Avşar *

Konya Technical University, Department of Geological Engineering, Konya, Turkey

ARTICLE INFO

Keywords:
Welded bimrock
Meso-scale direct shear test
Fragmentation fractal dimension
Block size distribution

ABSTRACT

Bimrocks have been rarely studied due to their inhomogeneous properties, challenges related to specimen preparation and tedious in-situ tests. This study was undertaken in an attempt to determine the shear strength parameters as well as the deformation behavior of a highly welded bimrock using laboratory meso-scale direct shear tests. In addition digital image processing analyses (DIP) and fragmentation fractal dimension (*DF*) calculations were made to quantify the geometrical and structural properties of the bimrock. It was concluded that the block size distribution of Sille bimrock is scale-invariant and shows fractal fragmentation. Moreover the block sizes have power-law distributions and there is evident skewness in normal distribution. The test results demonstrated that with the increase of volumetric block proportions (VBP), the internal friction angle (ϕ) of the bimrock increases whereas its cohesion (c) decreases. Strain softening behavior was observed after attaining the peak shear stress for all normal stresses and the VBP values. It is revealed that the normal stress is more effective than the VBP on the development of dilatation/contraction behavior. Lastly, the negative correlation between the *DF* and the peak shear stress indicated that the shear strength of the bimrock increases while the proportion of relatively small blocks in the specimen decreases.

1. Introduction

Block in matrix rock masses typically bear heterogeneous and chaotic features and show a wide distribution all over the world. Such rock masses are generally composed of rock blocks and/or fragments embedded in a matrix. These rock masses differ from each other in terms of geological genesis of the blocks and matrix material as well as the strength contrast of these two constituents. The mixtures of rocks composed of geotechnically significant blocks, within a bonded matrix of finer texture were defined as "Bimrock" by Medley (1994) for the first time. However, since then various researchers have made different definitions due to the fact that block in matrix rocks vary geologically, spatially and mechanically. In some types of bimrocks such as welded pyroclastics, agglomerates and fault breccias, the matrix may be a kind of rock material, while in other bimrocks such as severely weathered rocks, colluviums, glacial tills and soil/rock mixtures, the matrix may be soil-like. If the blocks and the matrix are not easily separated from each other and there is a significant degree of interlocking between these two constituents, such bimrocks are defined as "welded bimrock" (Lindquist, 1994; Sonmez et al., 2006a; Kahraman et al., 2008; Avşar, 2020). On the other hand, if there is no or very weak interlocking between the blocks and matrix, in that case they are called "unwelded bimrock" (Li et al., 2004; Kalender et al., 2014; Zhang et al., 2016). According to the preliminary bimrock classification, the contact strength between the matrix and blocks is accepted as approximately equal to the strength of the matrix for welded bimrocks. And, the contact strength is expected to be less than the strength of the matrix for unwelded bimrocks (Riedmüller et al., 2001; Altinsoy, 2006; Kalender et al., 2014). It should be noted there are bimrocks having different degrees of welding such as strongly welded or slightly welded. Hence, some new terminologies are used for bimrocks such as "bimsoil" a kind of unwelded bimrock including soil matrix (Kalender et al., 2014; Zhang et al., 2016), "rock and soil aggregate" (RSA) (Li et al., 2004; Wang et al., 2014) and "soil-rock mixture" (SRM) (Xu et al., 2007; Xu et al., 2011; Wang et al., 2016).

In recent years, bimrocks have started to attract the attention of researchers (e.g. Napoli et al., 2018; Napoli et al., 2020; Montoya-Araque et al., 2020) and becoming a popular research subject in line with the requirements of developing engineering applications. The bimrocks and/or mixed geological materials have some significant intrinsic properties and internal structures such as the amount of blocks, the

* Corresponding author.
E-mail address: eavsar@ktun.edu.tr.

https://doi.org/10.1016/j.enggeo.2021.106321
Received 23 September 2020; Received in revised form 28 July 2021; Accepted 2 August 2021
Available online 5 August 2021
0013-7952/© 2021 Elsevier B.V. All rights reserved.

strength of the constituents (matrix and blocks), the state of adhesion or welding between constituents, the surface roughness of the blocks which also form the shape of the contact surfaces (or interfaces) and block size distributions. The strength of bimrocks is controlled by these properties each with a different contribution rate. However, their specific influences have not yet been fully revealed today. Although studies on bimrocks have increased in recent years, it still needs improvements regarding the characterization of bimrocks and development and/or application of practical testing methods. Because of the difficulties in specimen preparation for laboratory testing and tedious in-situ testing, there are limited number of studies for determining the shear strength parameters of bimrocks.

There are some problems in performing the laboratory shear strength tests on bimrocks especially for bimsoils, RSA and SRM due to the difficulties in preparing high quality undistributed specimens in accordance with the standards and/or suggested methods. For this reason, Li et al. (2004) and Xu et al. (2007) designed and used an in-situ shear test device to determine the shear strength parameters of a SRM rock mass. Coli et al. (2011) on the other hand, inspired by these researches and redesigned the shear test setup and data recording system and improved new testing method called "BimTest". Moreover Kalender et al. (2014) proposed a preliminary Bim strength criterion and a generalized conceptual empirical approach for predicting the overall strength of unwelded bimrocks and bimsoils. The Bim strength approach includes empirical relations for prediction of cohesion (c) and the internal friction angle (ϕ) of unwelded bimrocks.

Some researchers have employed various laboratory and in-situ geotechnical testing methods in order to investigate the shear strength of bimrocks such as in situ direct shear tests on natural undisturbed samples (Zhang et al., 2016; Xu et al., 2011; Chu et al., 1996), in situ non-conventional shear tests (Li et al., 2004; Xu et al., 2007; Coli et al., 2011), laboratory triaxial tests (Lindquist, 1994; Goodman and Ahlgren, 2000; Sonmez et al., 2006a; Kahraman et al., 2008; Kalender et al., 2014; Altinsoy, 2006) medium-scale triaxial shearing system (Zhao and Liu, 2018) and large scale laboratory direct shear test (Zhang et al., 2020). In these studies, natural undisturbed bimsoil samples (Li et al., 2004; Xu et al., 2007; Zhang et al., 2016; Goodman and Ahlgren, 2000), artificial model samples (Lindquist, 1994; Kalender et al., 2014; Altinsoy, 2006; Zhang et al., 2020) and welded natural bimrock samples (Kahraman et al., 2008; Sonmez et al., 2006b) were subjected to the tests. It is understood that researchers have performed various testing methods on different type of bimrock samples such as artificial, natural undisturbed and large-scale. Different types of specimens and testing methods may yield incompatible results due to the scale effect, block/specimen size ratios and the welding degree between constituents of bimrocks. For instance, with the increase of the VBP, according to Lindquist (1994) cohesion decreases whereas in the study of Goodman and Ahlgren (2000) the cohesion increases. Furthermore, there are sudden drops in cohesion values when the block proportions lie in the range of 20% and 30% in Coli et al. (2011) and Xu et al. (2011) however the cohesion gradually decreases as the VBP increases in Wang et al. (2020). Thus, it will be very useful to investigate such rock masses with further studies involving different types of bimrocks and testing methods regarding the scale effect and to compare the results with the previous studies. As the number of studies increases, these bimrock masses will be better understood and the overall strength parameters of them may be more practically determined through simpler testing methods in the future.

Some precious historical semi-underground settlements were founded in Sille (Turkey) about 1500 years ago through carving out the pyroclastic deposits. In addition to these historical rock-hewn settlements, there are also modern structures on Sille bimrock due to the current urbanization. These pyroclastic deposits can be considered as highly welded bimrocks. On the other hand, the shear strength behavior of the Sille bimrock has not been investigated in any previous studies. Thus, determining some physical properties and the strength properties such as the c and the ϕ of Sille bimrock" is required. Therefore, in an attempt of filling the research gap in this area, Sille bimrock is selected as the material of this study for both being a good representative of a welded bimrock and as a material of a historical importance.

The main subject of this study is to investigate the shear strength behavior of a welded bimrock using laboratory direct shear tests on relatively large specimens (meso-scale). In addition, the effect of the VBP and fragmentation fractal dimension (*DF*) on the shear strength of the bimrock were evaluated thoroughly. The novelty of this study is to reveal the shear strength behavior of a welded bimrock by applying laboratory meso-scale direct shear test for the first time. On the other hand, digital image processing (DIP) and the *DF* studies were carried out in order to describe the physical and structural properties of the bimrock. The purpose of the study is to investigate the deformation behavior and shear strength parameters of the bimrock considering the VBP and the *DF* by performing laboratory meso-scale direct shear tests.

2. Description of Sille bimrock

In this study, a pyroclastic rock mass outcropped in historical Sille settlement in Turkey was studied. The pyroclastic deposits formed in a terrestrial environment with eruptions of the Late Miocene-Early Pliocene volcanism (Ozkan, 2017) The K—Ar ages of these rocks range from 11.95 to 3.35 Ma (Keller et al., 1977). These pyroclastic deposits are known as Sille agglomerate and attract attention due to the antique semi-underground openings carved in them and the stability problems encountered (Avşar, 2020).

Avşar, 2020 who studied on Sille agglomerate at the same location of this study found that the UCS of matrix varies between 2 and 7.6 MPa and the UCS of the andesite blocks varies between 5 and 22.5 MPa. These results suggested that there is a sufficient strength contrast between the blocks and the matrix. Hence Sille agglomerate coincides well with the definition of bimrock and is called as "Sille bimrock" regarding the geo-engineering description of the rock mass in this study. Sille bimrock is composed of different sized blocks and a fine grained matrix (Fig. 1a). Preparation of thin sections and optical microscopy analyses were conducted in the Mineralogy and Petrography Laboratory of Geological Engineering Department at Konya Technical University. It was identified that the matrix is tuff and the blocks are andesite through optical microscopy examinations. It was also observed that the porphyritic textured andesitic blocks contains quartzite phenocrysts, biotite, plagioclase and opaque minerals in a volcanic glass as matrix material. Based on the in-situ macro-structural observations, the andesite blocks have different shapes, degrees of angularity and quite variable surface roughness (Fig. 1a, b). Small blocks are usually semi-round, whereas large blocks have relatively high angularity (Fig. 1). It was clearly seen that there is no orientation in the distribution of the blocks on different surfaces of outcrops in different directions (Fig. 1). Block-to-block contacts are rare in the laboratory specimens and most of the blocks are interspersed in the fine matrix (Fig. 1b). On the other hand, block-block contacts are common in some places of the outcrops where especially large blocks are widespread (Fig. 1a). Bimrock samples of various sizes were gathered in the vicinity of the ancient rock-hewn settlements and were carried to the laboratory for experimental studies.

Bimrock samples containing relatively small sized andesite blocks were gathered in situ because of Sille bimrock contains various sizes of andesite blocks from small pebbles to large blocks (Fig. 1). Particular attention was paid to collect the bimrock samples having both blocks and matrix constituents together while the bimrock samples were gathering from the study area. Since Sille bimrock composed of two geomaterials having considerable strength contrast, many of the specimens broke into pieces or heavily disturbed while sawing. The major specimen preparation problem is the disturbance of cubical specimens when the saw bit contacts the block matrix interface during cutting. Careful sampling studies were exercised in sawing and smoothing to minimize mechanical damage to the testing specimens. Therefore, some special

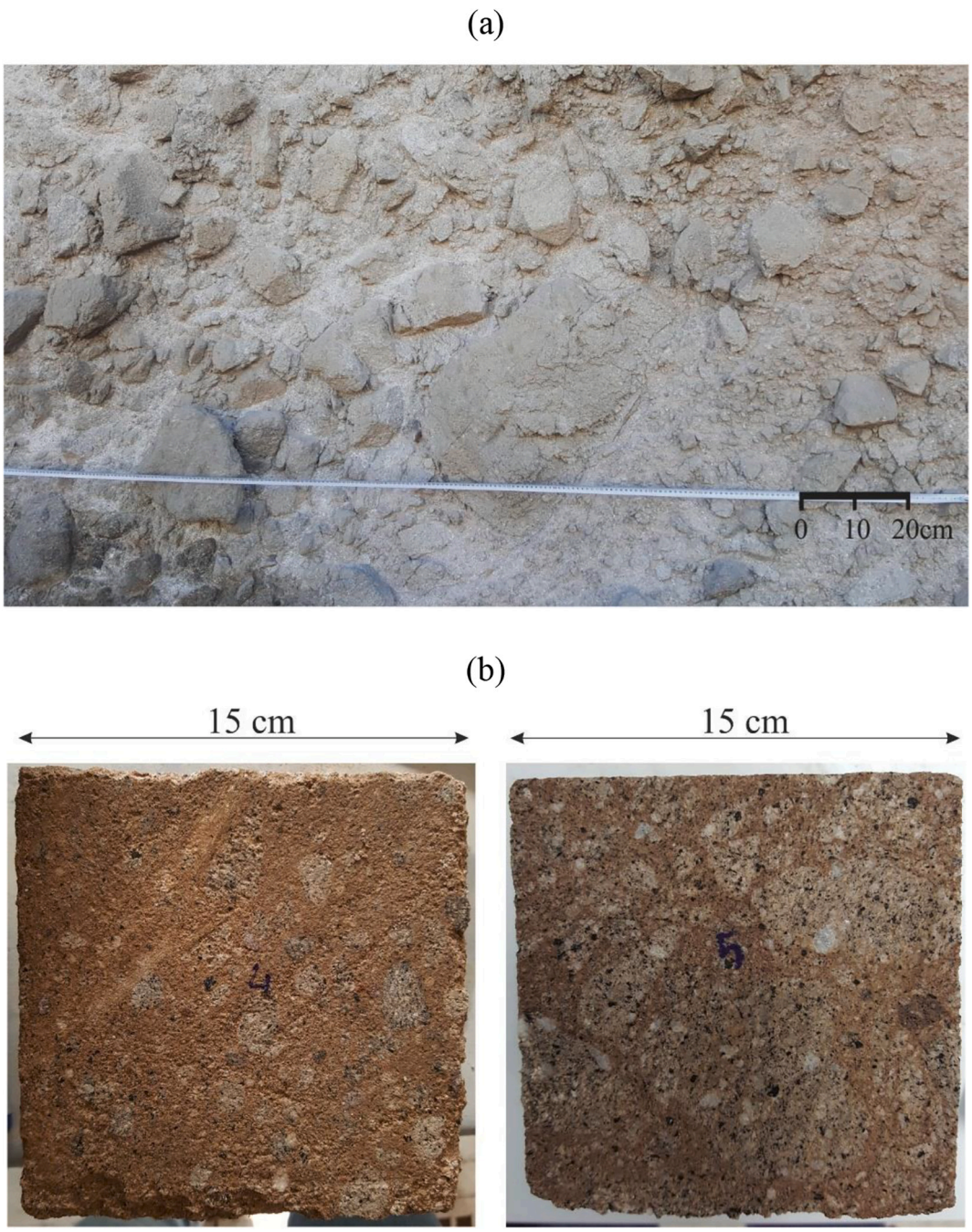

Fig. 1. (a) A close-up view of Sille bimrock including various sizes of blocks in fine grained matrix and (b) surface images of two cubical specimens including small and large blocks.

efforts were made during sampling procedures to minimize the disturbance problems. A disc shaped rock-cutting saw with 50 cm in diameter was used to prepare cubical specimens. The saw manufactured with fine diamond abrasives in its cutting edge was specially designed for soft rocks. The favorable sawing rate was detected after a number of trials while cutting specimens. Bimrock samples were strictly clamped on the sawing table in order to prevent the effect of vibration on the sample during cutting processes. All samples were sawed in wet conditions. Lastly, representative number of cubical specimens was extracted from the bimrock samples in the laboratory.

Since fragments (or blocks) of bimrocks may have any size and exist in all scales, the researchers may quite likely want to find the answer of that question: Which size of the fragments should be assumed as the minimum size of blocks on any scale? The fragments smaller than that size have a negligible effect on the geo-engineering properties of the bimrock and are going to be considered as matrix material. Therefore, a threshold value needs to be determined between the blocks and the matrix. The block/matrix threshold value is determined based on the scale of engineering interest. Medley (1994) proposed a block/matrix threshold related to the scale of engineering interest by a characteristic engineering dimension (L_c) such as the thickness of a landslide, the square root of a site area $\sqrt{A}$, the height of an excavation, the tunnel diameter, the footing width, the diameter of a core specimen etc. Medley (1994) concluded that the largest possible block in Franciscan melange at any scale of interest is about equivalent to $\sqrt{A}$ in size. However, since more than 99% of blocks are smaller than $0.75\sqrt{A}$, this size is defined as the largest reasonable block size (d_{max}) by Medley (1994). Thus, Medley (1994) and Medley and Lindquist (1995) suggested that the block/

matrix threshold is $d_{min} = 0.05L_c$ and the largest block, d_{max}, is $0.75L_c$. For instance, while Xu et al. (2008) assumed the root square of the area of the study zone as Lc, Xu et al. (2011) and Coli et al. (2011) used the height of the direct shear test specimen and the maximum length of the specimen as Lc, respectively.

In the present study, all specimen preparation studies were carried in accordance with the procedures of ASTM D5607 (2014) in the laboratory. A total of 15 cubical specimens with dimensions of 15x15x15 cm were prepared for direct shear tests in the laboratory. The digital image processing results indicated that there are differences between the maximum sizes of blocks in-situ and in cubical and core specimens. The theoretical d_{max} of the cubical specimens is equal to $\sqrt{A}$ and $A = 225$ cm^2 (is the area of one face of cubical specimen) and $d_{max} = 15$ cm for this study. This is a theoretical size and blocks with 15 cm in diameter were not observed in the cubical specimens in this study. The d_{max} suggested by Medley (1994) corresponds to quite large blocks for the laboratory specimens. If the cubical specimens contain blocks with $d_{max} = \sqrt{A}$ or $d_{max} = 0.75\sqrt{A}$, a very large part of the specimen would be occupied by a single block. In this case, the rock specimen may represent blocky rock features instead of a bimrock. On the other hand, the effect of the matrix on the overall strength will be neglected and the test results may not fully represent the bimrock. The maximum block size in the specimens and relative frequency of large blocks are considered in this study. The feret diameter of the largest block encountered in the cubical specimens is 8.5 cm, and the blocks with feret diameters between 6.75 cm and 8.50 cm constitute only 2% relative frequency of the total blocks. In other words, more than 98% of the blocks are smaller than $0.45\sqrt{A}$. Accordingly, $d_{max} = 0.45\sqrt{A}$ is defined as the largest reasonable block size ($d_{max} = 0.45*15 = 6.75$ cm) in this study. In addition, the influence of the largest blocks, which are already few in number, on the tests results was examined and any extra dispersion or repeatability did not observed in the experimental results.

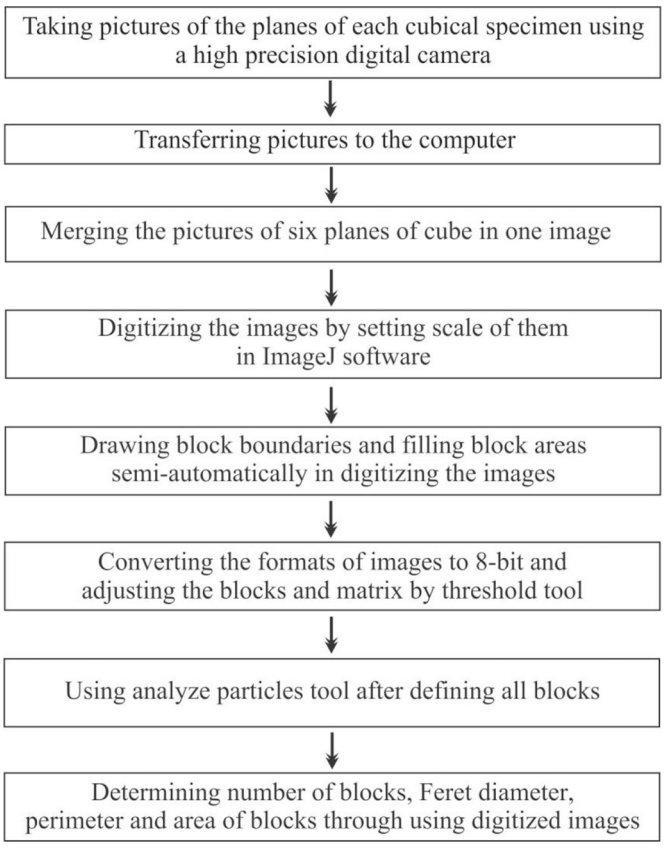

Fig. 2. Process flow diagram of DIP studies of Sille bimrock.

2.1. Digital image processing (DIP)

In recent years, digital image processing (DIP) is a frequently used technique in order to digitize the internal structure of geomaterials. Besides, the fractal dimension theory and fractal geometry calculations are used for quantifying the inhomogeneous deposits such as bimrocks, soil rock mixtures and fracture networks as a practical and reliable method (e.g. Feder, 1988; Gimknez et al., 1997; Ghanbarian et al., 2016; Ghanbarian et al., 2019). In this study, various block properties of Sille bimrock were determined using the DIP and the fractal dimension calculations were made on data obtained from the DIP studies.

With using DIP, it is possible to define shape characteristics and distribution of grains and/or fragments within geomaterials. Furthermore, DIP provides to determine area of the fragments in 2-dimesion (2D) on the digitized images. DIP includes the removal of noise, contrast enhancement, recovery, segmentation and characteristic extraction of images (from camera, vidicon, scanner, CT machine and tracing papers etc.) through computers (Xu et al., 2008). It is important to calculate the aerial block proportion (ABP) and volumetric block proportion (VBP) of bimrocks or rock block proportions (RBP) of SRM, since there are strong correlations between the ABP/VBP/RBP and the strength properties of bimrocks.

In order to describe the processes more clearly, the flow diagram of DIP studies of Sille bimrock is given in Fig. 2. The surface images of bimrock specimens were obtained by taking high-resolution photographs of faces of cubical specimens. The photographs of six faces of a cubical specimen were taken after the cubical specimens were prepared and cleaned and then uploaded to the computer. However, the color contrast adjustment could not made properly between the blocks and the matrix because they have very low color contrast. Therefore DIP analyses were conducted via "Fiji-ImageJ" (Schindelin et al., 2012) computer software in order to separate blocks from the matrix precisely and remove the noises from the images. The photographs of six faces were merged in one image and then the dimension of this digital image was converted from pixels to the actual dimensions in ImageJ (Fig. 3). Then, the block boundaries were outlined with drawing tool one by one and block areas were filled with black color on these digitized images (Fig. 3). The formats of all the images of cubical specimens were converted to 8-bit and the blocks and matrix were adjusted by threshold tool. Lastly, analyze particles tool was run to determine the block properties.

Some properties of blocks such as perimeter (P), area of blocks (A), apparent Feret diameter and apparent number of blocks (B_N) were determined through using digitized images. The Feret diameter is a measure of an object size along a specified direction. Usually, it can be described as the distance between the two parallel planes restricting the object perpendicular to that direction. It is also known as the caliper diameter, referring to the measurement of the object size with a caliper. The Feret diameter is commonly used in the particle size analysis. For instance, it is applied to projections of a three-dimensional (3D) object on a 2D plane. In such cases, the Feret diameter is defined as the distance between two parallel tangential lines rather than planes (Merkus, 2009; Wikipedia, 2021). Since Avşar, 2020 determined that the ratio of Feret diameter to minimum Feret diameter of most of the blocks within Sille bimrock are less than 1.5, it is assumed that the blocks have similar sizes in different aspects in 2D and 3D. Based on the finding related equi-dimensional property of blocks areal block proportions of each core and cubical specimens were calculated and these values were assumed equal to the VBP. The VBP values of specimens vary over a wide range (from 11% to 50%) indicating that Sille bimrock is highly heterogeneous. The B_N of the cubical specimens vary between 56 and 145 and these numbers reveal that the specimens contain significant numbers of blocks.

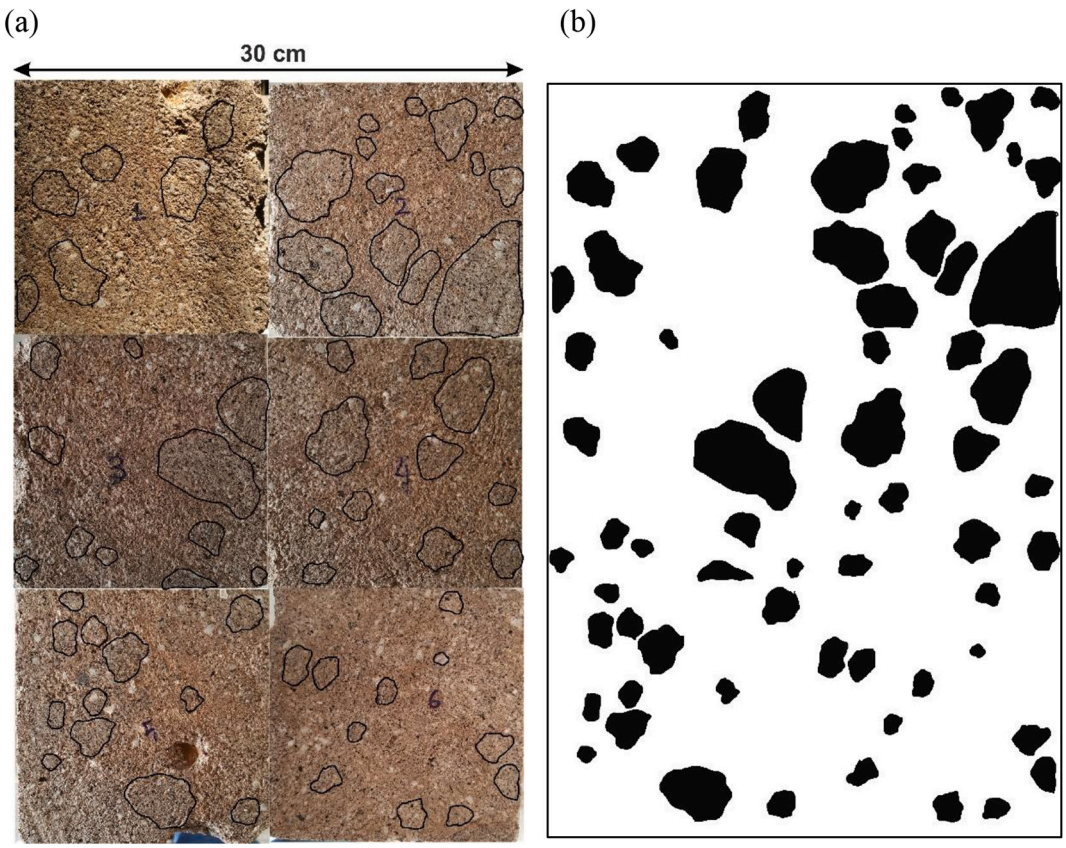

Fig. 3. Digitizing images of cubical specimens (a) merging the images of six faces of cube and drawing the outlines of the blocks (b) adjusting the threshold between blocks and matrix.

2.2. *Fragmentation fractal dimension and block size distribution of bimrock*

Fragmentation processes by means of e.g. weathering, volcanic eruptions and erosion have occurred or are still occurring in many geological environments. Many fragmented geo-materials are exposed by these processes. It is known that many geographical objects (e.g. lakes, islands) and geological materials (e.g. granular materials, blocks in bimrock, pyroclastics) in nature have the property of scale invariance. Hence size distribution of these materials are quantified by using fractal dimension theory (Mandelbrot, 1982). The empirical relation between number and size gives the definition of fragmentation fractal dimension (*DF*).

The number-size distributions of lakes and islands correspond the fractal property. Mandelbrot (1982) revealed that the size distribution of a population of islands is inherently a consequence of fractal fragmentation. Mandelbrot (1982) proposed Eq. 1 to quantify fragmentation by developing the fragmentation fractal dimension (*DF*) via Eq. 1.

$$N(R > r) = cr^{-DF} \quad (1)$$

Where $N(R > r)$ is the cumulative frequency of fragments with a linear dimension R (radius, diameter, perimeter etc.) greater than a given comparative size r and the exponent *DF* is the *fragmentation fractal dimension*, and c is a constant coefficient related to the maximum size. The fractal dimension derived from Eq. 1 is a measure of size-number relationship of the fragmentation of a population (Hyslip and Vallejo, 1997). Thus, it is concluded that there exists a straightforward relationship between the power-law size distributions and fractal phenomena.

Medley (1994) examined the areas range between 0.01 m^2 and 1000 km^2 containing different size of blocks in Franciscan melange and found that melange bimrocks are scale-invariant. In this study, Feret diameters of 633 blocks in four different areas (A) were measured to determine whether the block size distribution of Sille bimrock is scale-invariant. Two of these areas are outcrops of Sille bimrock having areas of A = 1.35 m^2 and A = 1.80 m^2. Feret diameters of blocks were measured on the scaled photographs of these two outcrops using DIP. The rest of the blocks were measured from DIP images of a cubical (A = 0.15 m^2) and a core specimen (A = 0.03 m^2). The Feret diameters of blocks were divided by the square root of the area ($\sqrt{A}$) containing the blocks to get dimensionless block size distributions at various scales. In order to demonstrate block distributions for different scales, log-log plots of "relative frequency vs. Feret diameter/$\sqrt{A}$" were obtained (Fig. 4). It can be seen from Fig. 4 the block size distributions are similar in appearance and they tend to distribute similarly. It could be concluded that the block

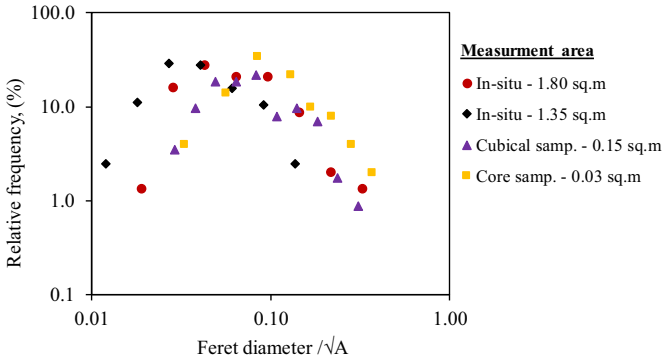

Fig. 4. Log-log histogram of Feret diameter/$\sqrt{A}$ to Relative frequency showing block size distribution of 633 blocks detected in different measurement areas in Sille bimrock.

size distribution of Sille bimrock is scale-invariant and shows fractal distribution.

Some researchers who investigated fragmented geo-materials including bimrocks have determined the *DF* (e.g. Medley, 1994; Hyslip and Vallejo, 1997; Coli et al., 2011; Mahdevari and Maarefvand, 2018). There are limited number of studies (Xu et al., 2007; Mahdevari and Maarefvand, 2018; Avşar, 2020) on the relations between the strength properties of bimrocks and the *DF*. Mahdevari and Maarefvand (2018) and Avşar, 2020 studied the effect of *DF* on deformation modulus and UCS of bimrocks. Xu et al. (2007) stated that shear strength parameters of rock block mixtures might be influenced by grain size distribution. However, Xu et al. (2007) studied the effect of grain size distribution characteristics but they did not calculate the *DF* to quantify the grain size distribution. Indeed, the relationship between the *DF* and the *shear strength behavior* of a welded bimrock has not been investigated in any previous study. In this study, fragmentation fractal dimension (*DF*) studies were conducted on cubical specimens subjected to direct shear tests. The influence of the *DF* on the shear strength behavior of the Sille bimrock was assessed in section 5.2.

The relationship between "Cumulative frequency" and "Feret diameter" of blocks was obtained for each cubical specimen. Then, these equations were simply used to determine the *DF*. As a representative example, a log-log graph of "N, Cumulative frequency" vs. "r, Feret diameter of block" of a specimen is presented in Fig. 5. The relationship in Fig. 5 is given in Eq. 2. The exponent of this equation is the *DF* and can be seen in Eq. 3. The *DF* values of the 15 cubical specimens were found from the relationships to log-log graphs of "N, cumulative frequency" vs. "r, Feret diameter" for each one. According to the results, the DF values range between 1.63 and 2.57.

$$y = 148.55 \times^{-1.85} \tag{2}$$

$$DF = 1.85 \tag{3}$$

Skewness is a measure of the asymmetry or distortion of the distribution of a variable. A perfectly symmetric distribution always has zero skewness. Accordingly, a distribution is regarded as skewed if it is leaning to the right or the left. The frequency distribution of Feret diameter of blocks was obtained for each cubical specimen. In addition, the generalized histogram of the block size frequency distribution of all blocks within the 15 cubical specimens is given in Fig. 6. It is concluded that all of the block size distributions are characterized by pronounced skewness in normal distribution. The distribution in the histogram in Fig. 6 has a positive skewness implies that the distribution is skewed to the right. The geometric mean is a special type of average or mean which signifies the central tendency or typical value of a set of values. The geometric mean is mostly used for a set of numbers whose values are non-linear or exponential. The arithmetic mean is usually used to find

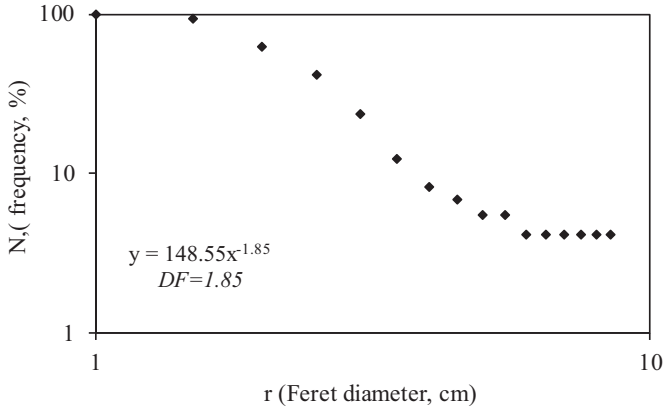

Fig. 5. Relation between "Frequency" and "Feret diameter of block" of a cubical specimen.

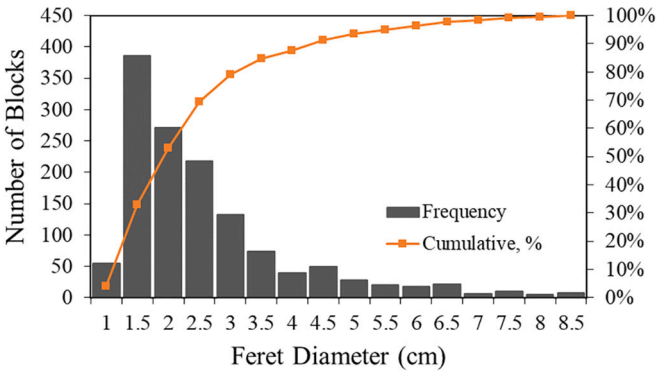

Fig. 6. Distribution of Feret diameters of all blocks within 15 cubical specimens.

central tendencies but it is effected by the values that are very much larger or smaller than most of the values (outliers). Geometric mean is more favorable to find central tendency of a set of values with skewed distribution. Since the block size distribution of Sille Bimrock is non-linear and skewed, the geometric mean was used to obtain the mean value of Feret diameters of all blocks. According to the results, the mean value of Feret diameters of all blocks is 2.04 cm. Blocks with Feret diameters smaller than 2.04 cm were classified as small blocks and those larger than this value as large blocks. As it is well kown, the increase in the *DF* indicates increasing in smaller blocks or a decrease in block sizes, relatively. In this study, it is determined that the *DF* values of the specimens including mostly large blocks are lower than those containing a great number of small blocks compatible with the concept of fractality.

3. Laboratory meso-scale direct shear tests

Standard test method (ASTM D5607–95) for performing laboratory direct shear strength tests of rock specimens under constant normal force was performed on cubical specimens of Sille bimrock.

3.1. Testing apparatus and specimen preparation

A direct shear test system (Fig. 7a) manufactured by Wille Geotechnik (2020) was used to determine the shear strength of bimrock specimens. There is a closed loop servo control shear apparatus in the direct shear test system. The apparatus includes a special frame construction consisting of two stiff frames for vertical force and shear force, combined in a special configuration to avoid friction and torque.

The maximum load capacity of both axial and shear force is 500 kN and the robust constructed frame has a high stiffness. The complete test system is fully automated and controlled by GEOsys software (Wille Geotechnik, 2020). The 150*150*150 mm cubical bimrock specimens were tested by this test system. A strong plaster with a 48-h strength of 36 MPa was used as encapsulating material. The specimens were fixed with screw holders (Fig. 7b) and then they were firmly potted in the shear boxes with plaster (Fig. 7c). The plaster and holders were used when placing specimen both in upper and lower boxes. The specimens with similar VBP values were subjected to shear tests in the same test set. It was observed that the failure surface in all tests was very close to horizontal with some tortuosity. Some observations made on the failure surfaces to determine the number and size of the blocks inclusions and the VBP values of the failure surfaces. However, after almost all tests, the boundaries of the blocks on the failure surfaces could not be followed due to the wearing of failure surfaces under severe friction. The blocks on the failure surfaces are not clear as it can be seen from the two typical images of the failure surfaces given in Fig. 8. In addition, spreading of crushed grains on the failure surfaces obscured the color contrast between the blocks and the matrix. The low color contrast is also one of the

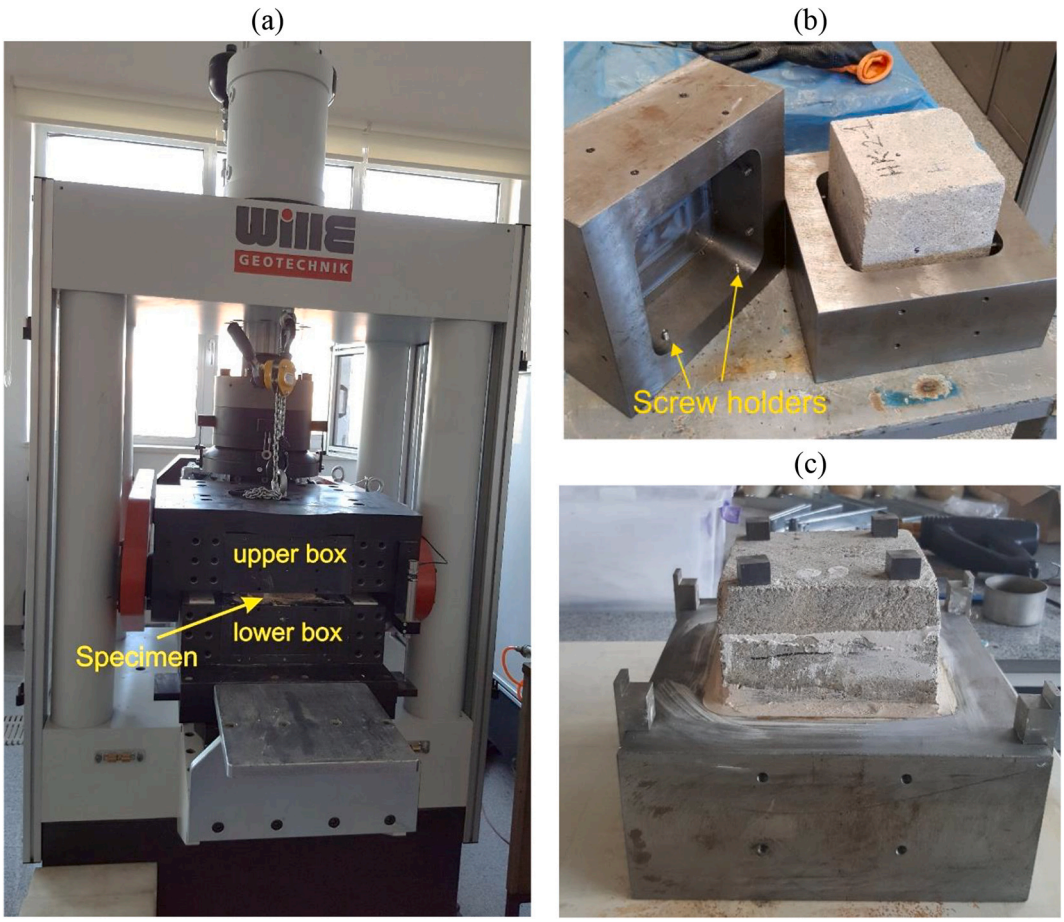

Fig. 7. (a) Direct shear test system, (b) lower and upper shear boxes and the specimen fixed with screw holders and (c) plaster-encapsulated specimen in lower box.

Fig. 8. Failure surfaces of two cubical specimens subjected to direct shear tests.

reasons for this fact. Although not very clear, both blocks and matrix material were observed on the failure surfaces.

3.2. Shear deformation behavior and shear strength of bimrock

For all normal stresses and the VBPs, strain softening occurred after attaining the peak shear stress and then the shear stress remained steady by reaching residual strength (Fig. 9a, c). According to the direct shear tests results (Table 1), the peak c and ϕ of bimrock specimens range from 264 to 894 kPa and from 24^0 to 41^0, respectively. The residual c and ϕ values of these specimens range from 121 to 262 kPa and from 23^0 to 37^0, respectively (Table 1). It should be noted that the decrease of the shear stress after reaching peak strength was greater than those of the specimens having high VBP values (Fig. 9a,c).

The curves of vertical displacement versus shear displacement were drawn to assess the deformation behavior of Sille bimrock. The displacement curves of specimens having VBP values of 15% and 45% were plotted in Fig. 9b, d as representative graphs. The positive axis of the vertical displacement is selected for dilatancy and the negative part for contraction. Dilatation rather than contraction is observed during the shearing process mostly under low normal stresses and for all VBP values. In other words, with increasing the normal stress, the positive

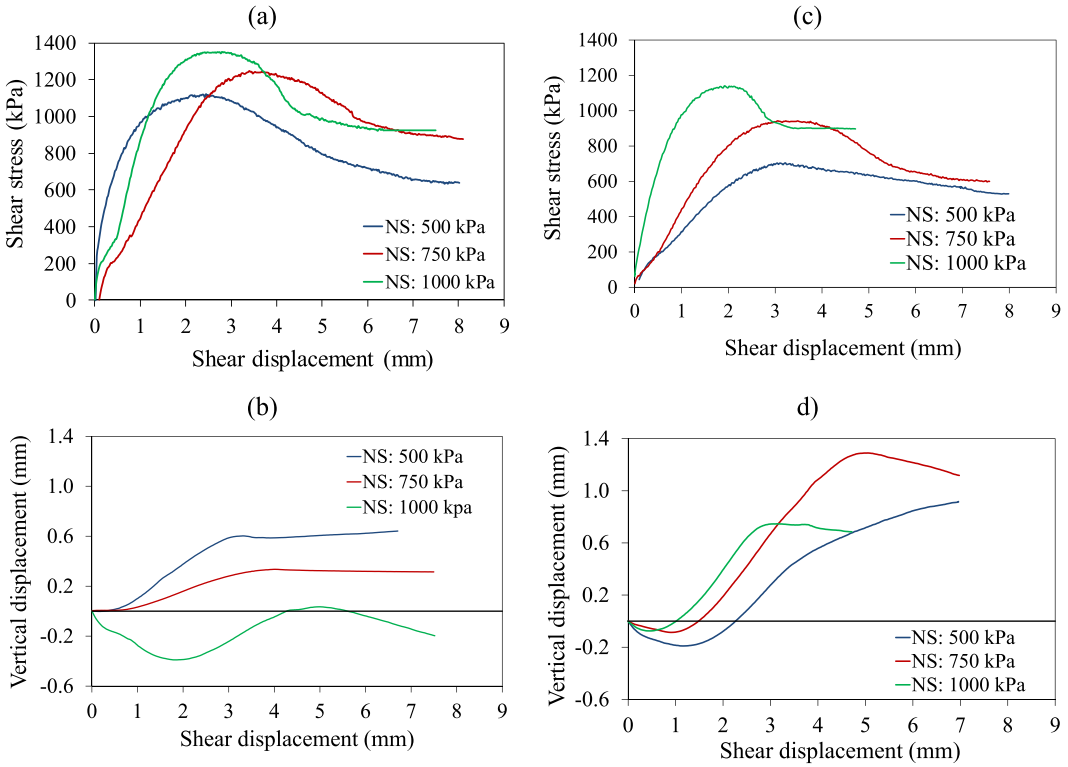

Fig. 9. "Shear stress-shear displacement" and "vertical displacement-shear displacement" relationships of (a, b) the specimens having 15% VBP and (c, d) the specimens having 45% VBP.

Table 1
Peak and residual ϕ and c values obtained from direct shear tests.

Sample No.	VBP of 3 specimens (%)	Peak ϕ (^{0})	Residual ϕ (^{0})	Peak c (kPa)	Residual c (kPa)
DS-1	(15),(14),(15)	24	29	894	262
DS-2	(22),(25),(25)	26	33	560	187
DS-3	(30),(31),(28)	29	23	368	156
DS-4	(37),(38),(35)	38	33	264	124
DS-5	(45),(47),(43)	41	37	275	121

vertical displacement decreased gradually. On the other hand, the amount of dilatation increases with increasing VBP values. While the vertical displacement of the specimen with 15% VBP reached a maximum value of 0.6 mm, the specimen with 45% VBP increased up to 1.3 mm (Fig. 9b, d).

For the specimen with 15% VBP (Fig. 9b) under 1000 kPa normal stress, contraction occurred until 2 mm shear displacement and then dilatation is observed up to 5 mm shear displacement with reaching the specimen almost the first height. Finally, until the end of the test, the contraction behavior was observed once again. On the other hand, there was no contraction for the specimens with %15 VBP subjected to normal stresses of 500 kPa and 750 kPa (Fig. 9b). Dilatation is in question until the horizontal displacement reaches approximately 3–4 mm for these two specimens. As the shearing continues from that point, the volumetric change of these two specimens were almost constant.

According to the curves of the specimens with 45% VBP (Fig. 9d), there are small amounts of contraction along with the negative vertical displacements ranging from 0.07 mm to 0.19 mm. And subsequently, dilatations with a minimum of 0.8 mm (under 1000 kPa of NS) and a maximum of 1.3 mm (under 750 kPa of NS) positive vertical displacement were achieved as shear displacement increased. The specimens with 25% VBP mainly indicated dilatation rather than contraction behavior for all normal stresses (Fig. 10 b,d,f). Very low vertical displacements were observed for the specimen 30% VBP subjected to 1000 kPa normal stress (Fig. 10f). The other specimens with 30% VBP under 500 and 750 kPa normal stresses have low contraction but higher amounts of dilatation (Fig. 10b,d). There was about 0.35 mm vertical displacement providing contraction for 37% VBP specimen under 1000 kPa normal stress (Fig. 10f).

In each graph in Fig. 10a,c and e "shear stress"-"shear displacement" curves of the specimens are presented under the same normal stress but with different VBP values. One can clearly see from these responses that the differences in the peak and the residual strengths are significantly influenced by the variations in the VBPs. This effect is more pronounced for the specimens subjected to low normal stress (Fig. 10a). For instance, when the VBP increases from 15% to 45% under the normal stress of 500 kPa, the amount of reduction in peak shear stress is 36% (see Fig. 10a). This rate decreases to 33% under the normal stress of 750 kPa whereas it drops 23% under 1000 kPa (see Fig. 10c and e).

In contrast to most of the previous studies (Zhang et al., 2020; Xu et al., 2011; Zhao and Liu, 2018; Li et al., 2004), the specimens with 15% VBP present the highest shear for all normal stress conditions (500, 750 and 1000 kPa, see Fig. 10a,c,e). Since these curves are relatively quite close to each other (see Fig. 9a), these specimens have the lowest $\phi_{peak} = 24^0$, while the peak and the residual cohesions are the highest such as $c_{peak} = 894$ kPa and $c_{residual} = 262$ kPa, respectively (Table 1). Looking at the curves of the specimens with 30% and 37% VBP, they have the lowest shear. The peak ϕ values ($\phi_{peak} = 29^0$ and $\phi_{peak} = 38^0$, Table 1) of these specimens are relatively high but still lower than that of the specimen having 45% VBP ($\phi_{peak} = 41^0$).

Normal stress is more effective than that of the VBP on vertical displacement (Fig. 10 b,d,f) and consequently of dilatation and/or contraction behavior. The amount of dilatation decreased as the normal stress increased from 500 kPa to 1000 kPa. The contraction behavior is mostly observed in some specimens subjected to 1000 kPa normal stress (Fig. 10f) whereas the dilatant behavior is more observed for relatively lower normal stresses (Fig. 10b, d). On the other hand, the effect of the

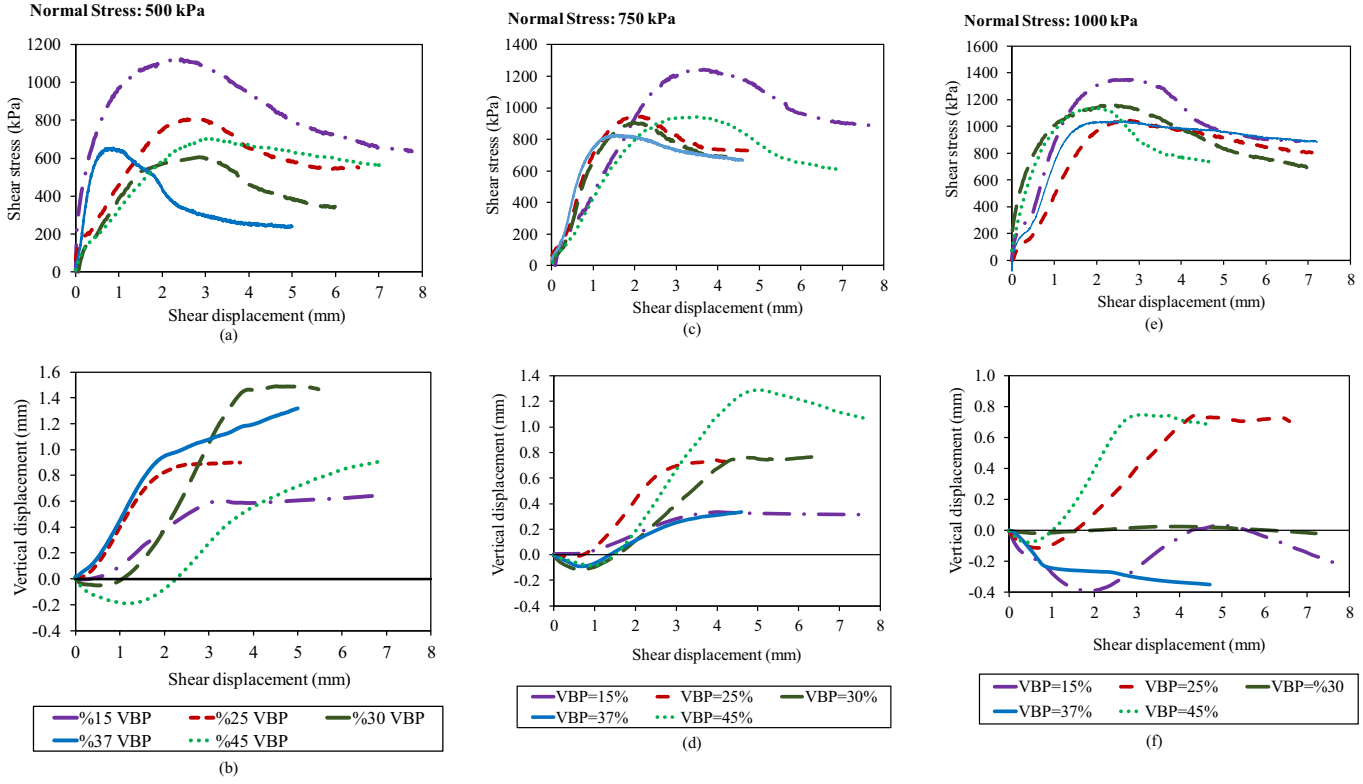

Fig. 10. Shear stress vs. shear displacement curves (a,c,e) and vertical displacement vs. shear displacement curves (b,d,f) of specimens of specimens having different VBP values under the normal stresses of (a,b) 500 kPa, (c,d) 750 kPa and (e,f) 1000 kPa.

VBP on the vertical deformation is ambiguous and therefore secondary in terms of importance to the normal stress. Nevertheless, a general trend was observed which demonstrated the increase in the amount of dilatation as the VBP increased (Fig. 10b,d,f).

In order to demonstrate the effect of the VBP on the shear strength parameters more clearly, the failure envelopes according to the peak shear stresses of the specimens with different VBPs are presented together in the same graph (Fig. 11). According to these failure envelopes and the c and ϕ determined from them (Table 1), it is clear that the c decreases and the ϕ increases as the VBP increases. While the increment in the internal friction angle up to 30% VBP is not prominent, it is more pronounced for the VBP values higher than 30%. Besides, the change interval of the residual c and ϕ values was determined to be relatively narrow. The relationships between the VBP and the shear strength parameters (c, ϕ) were worked through in section 5.

4. Discussion

4.1. Relations between the VBP and the shear strength parameters

In this study, the shear strength parameters (c and ϕ) as well as deformation characteristics of a volcanic welded bimrock were determined and assessed by performing meso-scale direct shear tests. The results reveal that the ϕ increases and the c decreases with increasing the VBP values obtained from these tests (Fig. 12). An increase in the VBP means that the contact surface (or the number of contact points) between the blocks and the matrix augments. Since the matrix-block interfaces are quite likely the weakest loci of welded bimrocks (Medley, 1994; Sonmez et al., 2006a; Sonmez et al., 2016) increasing the amount of block-matrix interfaces can be associated with decreasing of cohesion. The VBP decreases the c due to the increment of the block-matrix interfaces that weaken the bimrock. On the other hand, the internal friction angle increases probably because of the enhanced tortuosity of the rupture surface.

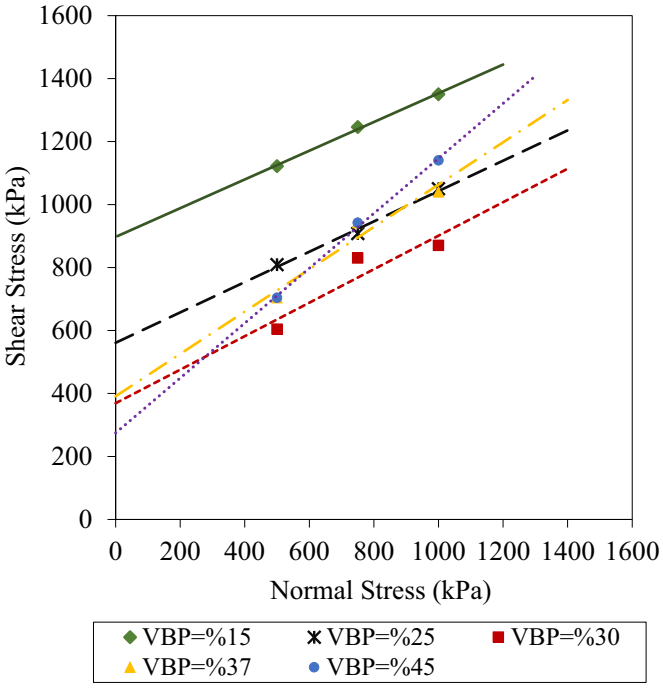

Fig. 11. Variation of the peak shear strength failure envelopes of all bimrock specimens having different VBPs.

As it is pointed out in section 1, the matrix material of Sille bimrock is a kind of weak rock and the constituents of the bimrock are welded unlike the other commonly studied bimsoils and/or soil rock mixtures.

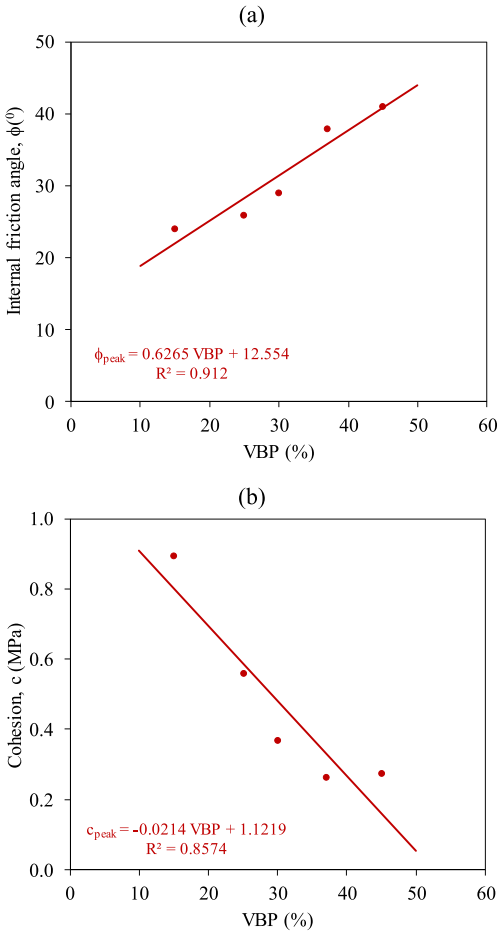

Fig. 12. Relationships between (a) the VBP and internal friction angle and (b) the VBP and cohesion.

Except for a limited number of studies (Lindquist, 1994; Sonmez et al., 2006a; Kahraman et al., 2008) the bimrocks studied in the literature are slightly welded or unwelded. Therefore, that difference has always been taken into consideration when comparing the results obtained from this study with those obtained from other studies. The impact of the VBP on the strength characteristics of bimrocks has been evaluated in some of the previous studies (e.g. Lindquist, 1994; Lindquist and Goodman, 1994; Coli et al., 2011; Mahdevari and Maarefvand, 2016).

Lindquist (1994) studied on the welded model melange specimens and revealed that the most of the shear failure surfaces followed the margins of the largest blocks. To form such tortuous path, the failure surface became increasingly rough with greater VBP values. Lindquist (1994) suggested that the increase in friction with growing the VBP can be attributed to the geometric effect of augmented tortuosity of failure surface. Lindquist and Goodman (1994) found that if the VBP increases, the cohesion decreases, the ϕ increases and modulus of deformation also increases. Sonmez et al. (2006a) briefly examined the relationships between the c, ϕ and the VBP of an artificial welded bimrock, but they did not make any interpretation on the reasons of these relationships. Besides, Kahraman et al. (2008) studied the relationship between the VBP and differential stress that obtained from triaxial tests of a welded breccia. In these two studies, no evaluation was made on the reasons for the change of the c and ϕ with increasing VBP values. On the other hand, Medley (1994) studied on slightly welded or unwelded bimrocks from Franciscan mélange and stated that the decrease in cohesion as the VBP increases due to the increase in the proportion of block-matrix interfaces. Similarly, Zhang et al. (2020) found that increase in the VBP resulting a considerable decrease in the cohesion of SRM from large-scale laboratory direct shear tests.

As mentioned before, only strain softening behavior is observed in all tests in this study. However, Zhang et al. (2020) observed strain softening for low VBP values and strain hardening for high VBPs under high normal stresses. Similarly, Coli et al. (2011) observed both strain hardening and softening responses. On the other hand, Zhao and Liu (2018) have obtained pronounced strain hardening responses in the most of the tests.

"The VBP" and "increment of ϕ" relationships determined in the previous studies and this study were presented in the same graph in Fig. 13. As it can be seen from this graph, the result obtained in this study is compatible with the results of previous studies in terms of increment of ϕ. All of the relationships in the graph have positive linear correlations and plots of them are located above the conservative trend line of Lindquist (1994). According to the plot of conservative trend from Lindquist (1994), the ϕ does not change for the VBP values of less than about 30% and greater than 75%. Unlike the conservative trend, there are remarkable changes in the increment of the ϕ for the VBP values less than 30% in this study and also in the study of Medley (2002) and Coli et al. (2011) (Fig. 13). Regarding that discrepancy, it may be an object of interest to investigate the change of the ϕ for the VBP lower than 30% and higher than 75% of different types of bimrock masses to achieve more precise results.

4.2. Relation between the DF and the peak shear stress

Bimrocks are composed of various size of rock blocks forming different block size distributions. Size distribution characteristics most likely effect the overall strength of such rock masses. The fractal dimension theory is a very practical and robust tool to define roughness and size distribution characteristics of the blocks. The c and ϕ were determined using the results of five direct shear tests and the specimens used in these tests have different *DF* values even if the values are close to each other. Thus, a single *DF* value corresponding to each c and ϕ pair could not be obtained. Therefore, the relationships between the *DF* and the peak shear stress of each direct shear test were investigated. Since the direct shear tests were conducted under the normal stresses of 500, 750 and 1000 kPa, the relationships between the *DF* and the peak shear stress were analyzed for these normal stresses. As it can be seen from Fig. 14, there are inversely proportional linear relationships between the *DF* and the peak failure stress with considerable values of coefficient of determination (R^2) for all normal stresses (Fig. 14). Data points in

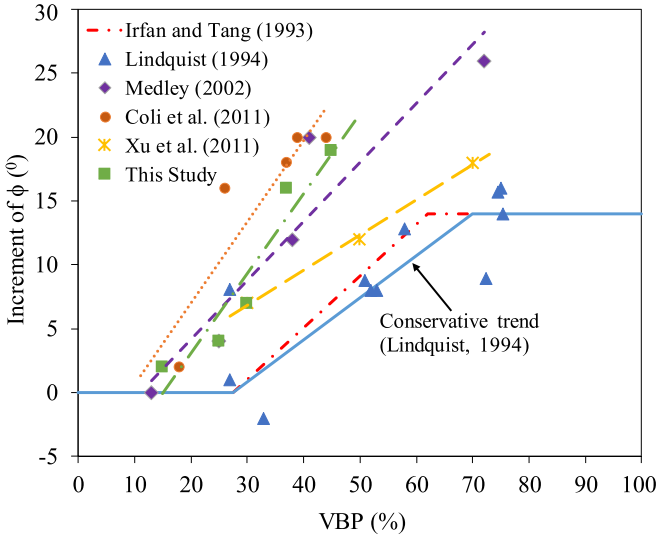

Fig. 13. Comparison of relationships between increments of the ϕ and the VBP determined in the previous studies and in this study (updated after Lindquist, 1994 and Xu et al., 2011).

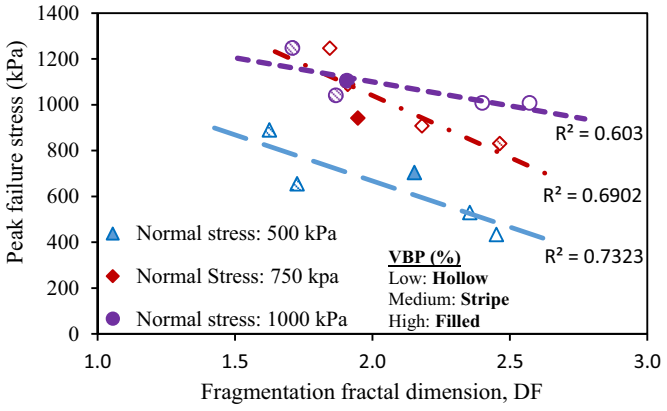

Fig. 14. Relationships between the *DF* and the peak failure stress for different normal stresses.

Fig. 14 were also arranged according to the VBP. As it can be seen from the graph, low VBP values indicated high DF values while medium and high VBP values indicated lower DF values. As explained in Section 2.2, increasing of the *DF* means increasing the amount of the small blocks in the specimen. It is thereby concluded that increasing in the amount of large blocks causes an evident increase in the shear strength of the bimrock. Similarly, Wang et al. (2020) concluded that the peak shear force increases with the increase of block sizes in bimsoils.

5. Conclusions

In this study, a series of meso-scale direct shear tests were performed on the bimrock specimens to investigate their strength and deformation characteristics. In addition, DIP studies and *DF* determinations were made to describe the block characteristics and block size distribution of the bimrock. The following conclusions can be drawn:

1. It is evident from the direct shear tests results, there is a positive linear relationship between the VBP and the ϕ with a considerable value of coefficient of determination ($R^2 = 0.912$). In contrast, inversely proportional linear relationship was found between the VBP and the cohesion ($R^2 = 0.857$).
2. The decrease in cohesion with increasing VBP is attributed to the weakening of the bimrock with the increasing of block-matrix interfaces that is the weakest component of the bimrocks. Another important conclusion is the ϕ increases due to the increasing rough block surfaces and tortuous contact surfaces between blocks and matrix.
3. The results demonstrated that the block size distributions of all specimens were characterized by pronounced skewness in normal distribution. Furthermore the block size distribution of the bimrock has scale-invariance and hence fractal property.
4. The results of almost all tests suggested that material's behavior is predominantly in strain softening mode, once the peak shear stress is reached. Dilatant behavior rather than contraction is observed during the shearing mainly under low normal stresses and for all VBP values.
5. The relationships between the fragmentation fractal dimension (*DF*) and the peak strength are inversely proportional and linear having significant R^2 values for all normal stresses. It is revealed that the increasing in the proportion of the large blocks leads a prominent increase in the shear strength of the bimrock.

Declaration of Competing Interest

The author of this paper declare that she has no conflict of interest.

Acknowledgements

This study was financially supported by Selcuk University Scientific Research Projects (BAP) (Project no. 17401137) (Konya, Turkey). The author would like to thank Prof. Dr. Kamil Kayabalı, Geological Engineer Deniz Yılmaz and Dr. Ferhat Habibzadeh (Ankara University) for their kind assistance during the laboratory studies. Special thanks to Dr. Hatice Ünal Ercan (Konya Technical University) for her kind help to carry out the optical microcopy analysis. The authors also acknowledge the anonymous reviewers for their constructive comments that led to improvements in the article.

References

Altinsoy, H., 2006. Matriks içinde blok içeren kayaların makaslama dayanımın belirlenmesi için fiziksel model esaslı bir araştırma. M.Sc.Thesis. Ankara, Hacettepe Univ (in Turkish).
ASTM, 2014. Annual Book of ASTM Standards-Soil and Rock, Building Stones, Section-4, Construction vol. 04.08. ASTM Publications, Philadelphia.
Avşar, E., 2020. Contribution of fractal dimension theory into the uniaxial compressive strength prediction of volcanic welded bimrock. Bull. Eng. Geol. Environ. 79, 3605–3619. https://doi.org/10.1007/s10064-020-01778-y.
Chu, B.L., Pan, J.M., Chang, K.H., 1996. Field geotechnical engineering properties of gravel formations in western Taiwan. Sino-Geotech. 55, 47–58.
Coli, N., Berry, P., Boldini, D., 2011. In situ non-conventional shear tests for the mechanical characterisation of a bimrock. Int. J. Rock Mech. and Min. Sci. 48 (1), 95–102. https://doi.org/10.1016/j.ijrmms.2010.09.012.
Feder, J., 1988. Fractals. Plenum. Springer US.
Ghanbarian, B., Hunt, A.G., Daigle, H., 2016. Fluid flow in porous media with rough pore-solid interface. Water Resour. Res. 52, 2045–2058. https://doi.org/10.1002/2015WR017857.
Ghanbarian, B., Perfect, E., Liu, H.A., 2019. Geometrical aperture-width relationship for rock fractures. Fractals. 27 (1), 12. https://doi.org/10.1142/S0218348X19400024.
Gimknez, D., Perfect, E., Rawls, W.J., Pachepsky, Y., 1997. Fractal models for predicting soil hydraulic properties. Eng. Geol. 48, 61–83. https://doi.org/10.1016/S0013-7952(97)00038-0.
Goodman, R.E., Ahlgren, C.S., 2000. Evaluating safety of concrete gravity dam on weak rock Scott Dam. J. Geotech. Geoenviron. Eng 126, 429–442. https://doi.org/10.1061/(ASCE)1090–0241(2001)127:10(900).
Hyslip, J.P., Vallejo, L.E., 1997. Fractal analysis of the roughness and size distribution of granular materials. Eng. Geol. 48 (3–4), 231–244. https://doi.org/10.1016/S0013-7952(97)00046-X.
Kahraman, S., Alber, M., Fener, M., Gunaydin, O., 2008. Evaluating the geomechanical properties of Misis fault breccia (Turkey). Int. J. Rock Mech. Min. Sci. 45 (8), 1469–1479. https://doi.org/10.1016/j.ijrmms.2008.02.010.
Kalender, A., Sonmez, H., Medley, E., Tunusluoglu, C., Kasapoglu, K.E., 2014. An approach to predicting the overall strengths of unwelded bimrocks and bimsoils. Eng. Geol 183, 65–79. https://doi.org/10.1016/j.enggeo.2014.10.007.
Keller, J., Jung, D., Burgath, K., Wolf, F., 1977. Geologie undpetrologie des Neogenen kalkalkali-vulkanismus von Konya (Erenler Dağ-Alaca Dağ-Massiv Zentral-Anatolian). Geo. Jb.B 25, 37–117.
Li, X., Liao, Q.L., He, J.M., 2004. In-situ tests and a stochastic structural model of rock and soil aggregate in the three Gorges Reservoir area, China. Int. J. Rock Mech. Min. Sci. 41 (3), 702–707. https://doi.org/10.1016/j.ijrmms.2004.03.122.
Lindquist, E.S., 1994. The strength and deformation properties of melange. Ph.D.Thesis, University of California, 264.
Lindquist, E.S., Goodman, R.E., 1994. The strength and deformation properties of a physical model mélange. In: Proc. 1st north American Rock Mech. Symp., Austin, Texas, pp. 843–850.
Mahdevari, S., Maarefvand, P., 2016. An investigation into the effects of block size distribution function on the strength of bimrocks based on large-scale laboratory tests. Arab. J. Geosci. 9, 509. https://doi.org/10.1007/s12517-016-2499-2.
Mahdevari, S., Maarefvand, P., 2018. Experimental investigation of fractal dimension effect on deformation modulus of an artificial bimrock. Bull. Eng. Geol. Environ. 77, 1729–1737. https://doi.org/10.1007/s10064-017-1074-8.
Mandelbrot, B.B., 1982. The Fractal Geometry of Nature. W. H Freeman, San Francisco, California.
Medley, E., 1994. The engineering characterization of melanges and similar block-in-matrix rocks (BIMRock's). Ph.D.Thesis. University of California, p. 174.
Medley, E.W., 2002. Estimating Block size Distributions of Melanges and similar Block-in- Matrix Rocks (Bimrocks). Proceedings of 5th north American Rock Mechanics Symposium (NARMS), pp. 509–606.
Medley, E.W., Lindquist, E.S., 1995. The engineering significance of the scale-independence of some Franciscan melanges in California. In: Daemen, J.K., Schultz, R.A. (Eds.), Proceedings of the 35th US Rock Mechanics Symposium. Balkema, Rotterdam, pp. 907–914.
Merkus, G.H., 2009. Particle Size Measurements: Fundamentals, Practice, Quality. Springer.
Montoya-Araque, E.A., Suarez-Burgoa, L.O., Medley, E.W., 2020. Application of the tortuous surface method to stochastic analysis of bimslope stability. Bull. Eng. Geol. Environ. 79, 5329–5340.

Napoli, M.L., Barbero, M., Ravera, E., Scavia, C., 2018. A stochastic approach to slope stability analysis in bimrocks. Int. J. Rock Mech. Min. Sci. 101, 41–49.
Napoli, M.L., Milan, L., Barbero, M., Scavia, C., 2020. Identifying uncertainty in estimates of bimrocks volumetric proportions from 2D measurements. Eng Geol 278, 105831. https://doi.org/10.1016/j.enggeo.2020.105831, 5 December 2020.
Ozkan, M.A., 2017. Küçükmuhsine – Sulutaş (Konya batısı, Türkiye) Çevresindeki Karasal Neojen Çökellerinin (Geç Miyosen-Erken Pliyosen) Stratigrafisi. El-Cezerî J. Sci. Eng. 4 (3), 382–410 (In Turkish).
Riedmüller, G., Brosch, F.J., Klima, K., Medley, E.W., 2001. Engineering geological characterization of brittle faults and classification of fault rocks. J. Eng. Geol. Geomech. Tunn. 19, 13–19.
Schindelin, J., Arganda-Carreras, I., Frise, E., et al., 2012. Fiji: an open-source platform for biological-image analysis. Nat. Methods 9 (7), 676–682.
Sonmez, H., Altinsoy, H., Gokceoglu, C., Medley, E.W., 2006a. Considerations in developing an empirical strength criterion for bimrocks. In: 4th Asian Rock Mechanics Symposium. Retrieved from. http://bimrocks.com/bimsite/wp-content/uploads/2010/07/Sonmez-et-al-2006.pdf.
Sonmez, H., Gokceoglu, C., Medley, E.W., Tuncay, E., Nefeslioğlu, H.A., 2006b. Estimating the uniaxial compressive strength of a volcanic bimrock. Int. J. Rock Mech. Min. Sci. 43, 554–561. https://doi.org/10.1016/j.ijrmms.2005.09.014.
Sonmez, H., Ercanoglu, M., Kalender, A., Dagdelenler, G., Tunusluoglu, C., 2016. Predicting uniaxial compressive strength and deformation modulus of volcanic bimrock considering engineering dimension. Int. J. Rock Mech. Min. Sci. 86, 91–103. https://doi.org/10.1016/j.ijrmms.2016.03.022.
Wang, Y., Li, X., Zhang, B., Wu, Y., 2014. Meso-damage cracking characteristics analysis for rock and soil aggregate with CT test. Sci. China Technol. Sci. 57, 1361–1371. https://doi.org/10.1007/s11431-014-5578-1.
Wang, Y., Li, X., Zheng, B., Mao, T.Q., Hu, R.L., 2016. Investigation of the effect of soil matrix on flow characteristics for soil and rock mixture. Geotech. Lett. 6, 1–8. https://doi.org/10.1680/jgele.16.00085.
Wang, Y., Feng, W.K., Li, C.H., Hou, Z.Q., 2020. An investigation into the effects of block size on the mechanical behaviors of bimsoils using variable-angle shear experiments. Environ. Earth Sci. 79, 69. https://doi.org/10.1007/s12665-020-8812-0.
Wikipedia, 2021. Website. https://en.wikipedia.org/wiki/Feret_diameter (accessed 06.02.2021).
Wille Geotechnik. 2020 Website: https://www.wille–geotechnik.com/en/geotechnics _rock _direct shear testing_static _ systems.html, (accessed 15.08.2020).
Xu, W.J., Hu, R.L., Tan, R.J., 2007. Some Geomechanical Properties of Soil-Rock Mixtures in the Hutiao Gorge Area, China. Geotechnique. 57 (3), 255–264.
Xu, W.J., Yue, Z., Hu, R.L., 2008. Study on the mesostructure and mesomechanical characteristics of the soil-rock mixture using digital image processing based finite element method. Int. J. Rock Mech. and Min. Sci. 45 (5), 749–762. https://doi.org/10.1016/j.ijrmms.2007.09.003.
Xu, W.J., Xu, Q., Hu, R.L., 2011. Study on the shear strength of soil-rock mixture by large scale direct shear test. Int. J. Rock Mech. and Min. Sci. 48 (8), 1235–1247. https://doi.org/10.1016/j.ijrmms.2011.09.018.
Zhang, H.Y., Xv, W.J., Yu, Y.Z., 2016. Triaxial tests of soil-rock mixtures with different rock block distributions. Soils Found. 56 (1), 44–56. https://doi.org/10.1016/j.sandf. 2016.01.004.
Zhang, Z., Sheng, Q., Fu, X., Zhou, Y., Huang, J., Du, Y., 2020. An approach to predicting the shear strength of soil-rock mixture based on rock block proportion. Bull. Eng. Geol. Environ. 79, 2423–2437. https://doi.org/10.1007/s10064-019-01658-0.
Zhao, Y., Liu, Z., 2018. Study of material composition effects on the mechanical properties of soil-rock mixtures. Advan. Civ. Eng. 2018, 1–10. https://doi.org/10.1155/2018/3854727.